Structural change and heteroepitaxy induced by rapid thermal annealing of CaF_2 films on Si(111)

N. Mattoso,[a] D. H. Mosca, and W. H. Schreiner
Departamento de Física, Laboratório de Materiais, UFPR, Caixa Postal 19081, 81531-990 Curitiba-PR, Brazil

I. Mazzaro
Departamento de Física, Laboratório de Otica de Raios-X e Instrumentação, UFPR, Caixa Postal 19081, 81531-990 Curitiba-PR, Brazil

S. R. Teixeira
Laboratório de Filmes Finos, Instituto de Física, UFRGS, Caixa Postal 15051, 91501-970 Porto Alegre-RS, Brazil

W. A. A. Macedo and M. D. Martins
Laboratório de Física Aplicada, Centro de Desenvolvimento de Technologia Nuclear, 30161-970 Belo Horizonte-MG, Brazil

(Received 13 November 1997; accepted 6 March 1998)

In this article we show that heteroepitaxial CaF_2 films can be induced on Si(111) with a rapid thermal anneal. The change from preferentially oriented polycrystals to a single crystal with type-*B* epitaxy is visible by different structural techniques. The x-ray photoelectron spectroscopy results indicate the presence of a reacted layer at the CaF_2/Si interface with a pronounced increase of fluorine atoms at this interface. Transmission electron microscopy results show that big structural changes occur due to the thermal pulse. © *1998 American Vacuum Society.*
[S0734-2101(98)07004-3]

I. INTRODUCTION

The heteroepitaxial growth of CaF_2 on Si(111) has recently received much attention due both to fundamental interest and potential technological applications for the future such as very-high-speed integrated circuits (ICs) and optoelectronic devices.

In particular, CaF_2 is a material almost isomorphous to Si. At room temperature the lattice parameter mismatch between these two materials is only of 0.6%. Heteroepitaxial fluoride films grow on Si(111) in two possible orientations. Type-*A* growth occurs when the CaF_2 crystallographic orientation matches that of the substrate, while in type-*B* epitaxy, the orientation is rotated 180° around the surface normal $\langle 111 \rangle$ axis.[1] Ohmi *et al.*[2] showed that the role of the first layers through a so-called two-step growth method can be very effective for growing rotational twin-free CaF_2 films. The CaF_2/Si interface has attracted several efforts in fundamental research. Tromp and Reuter[3] found that a Ca silicide is formed at the CaF_2/Si interface in films deposited at 770 °C. Cho *et al.*[4] reported on a new method to grow CaF_2 films on Si(111), which exhibit type-*A* epitaxy with good crystalline quality, based on a heating ramp during the initial 5 min of the deposition at low temperatures. The epitaxial growth of CaF_2 at low deposition temperatures indicated that at up to 8 monolayers the type-*A* epitaxy are formed even when submitted to a subsequent thermal annealing at 600 °C for 30 min[2]. We found only one article about the use of rapid-thermal anneal (RTA) in the deposition of CaF_2 films grown on Si(111).[5] Singh *et al.*[5] have reported on films almost free of tensile planar strain and free of defects employing RTA *in situ* at the deposition. That exploratory work opens some questions about the crystalline structure of annealed films, the reasons for reduced planar strain and defects, as well as details of the CaF_2/Si interface.

In this article we show that a low film deposition temperature, followed by RTA *in situ*, leads to high quality type-*B* epitaxial CaF_2 films on Si(111).

II. EXPERIMENT

The CaF_2 films were deposited by sublimation of CaF_2 with a resistively heated tantalum crucible in a BALZERS UMS 500P ultrahigh vacuum (UHV) machine with a base pressure of 1×10^{-8} mbar. The film thickness was controlled by a quartz crystal microbalance. The nominal thickness for different CaF_2 samples was of 40, 150, and 300 nm and the deposition rate was stabilized at 0.1 nm/s. The substrates, commercial Si(111) wafers cut off-axis by 2.5°, were cleaned by dipping in HF immediately before loading. During deposition the substrates were kept at 300 °C. After deposition some of these samples were annealed *in situ* at 1000 °C for 1 min. The heating during the film deposition and during the flash was accomplished using a halogen lamp located at the back of the Si wafer.

We employed ω-scan rocking curve and asymmetrical χ scan x-ray diffraction geometries using Cu $K_{\alpha1}$ radiation to characterize the samples, as well as reflectometry measurements with grazing angle reflected x rays to probe the true thickness and interface roughness of the films. The CaF_2 interfaces were investigated *ex situ* with x-ray photoelectron spectroscopy (XPS) with Mg K_α radiation (1253.6 eV), us-

[a]Electronic mail: mattoso@fisica.ufpr.br

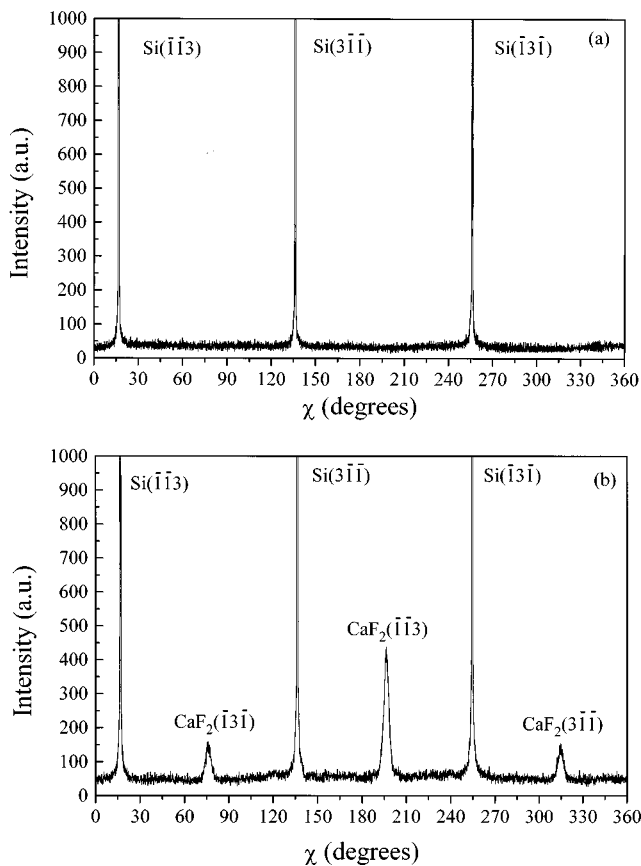

FIG. 1. Asymmetric χ scan of the (311) planes for a 40 nm CaF_2 thin films. (a) Diffraction for the unannealed film. (b) Result for the rapid thermally annealed film. The χ scans were obtained using a (111) channel-cut Ge four crystal monochromator, the radiation having a grazing incidence of 0.8° with respect to the sample plane. The detector was placed fixed at 56° with respect the incident beam and at 79.52° with respect to ⟨111⟩ direction, where the (311) diffraction is expected. The samples were rotated by 360° to record the signal.

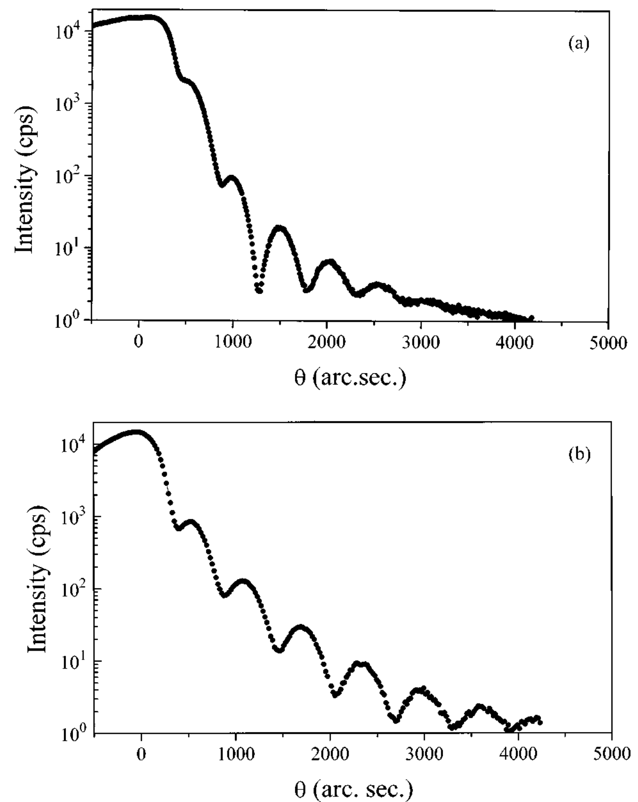

FIG. 2. X-ray reflectivity of 40 nm CaF_2 film deposited on Si(111). (a) Curve reflectivity profile of the sample without RTA while (b) is referent to the sample with RTA. These measurements were performed in a double axis diffractometer using a first crystal monochromator a Si(111) bulk crystal.

ing an UHV system with a base pressure of 2×10^{-10} mbar and a CLAM2 analyzer at 50 eV pass energy. Depth profiles were investigated using Ar^+ sputtering at 2.75 kV. The morphology and the microstructure of the samples were investigated by transmission electron microscopy (TEM) as well as selected area electron diffraction (SAED), using a JEOL 1200EX-II microscope operating at 120 kV.

III. RESULTS

Figure 1 shows an asymmetric χ scan of the samples probing the (311) diffraction lines of CaF_2 and Si. In Fig. 1(b) the label on the peaks helps to show that the epitaxy of the CaF_2(40 nm) film with RTA is type *B*, that is, the lattices of CaF_2 and Si are rotated relatively to the ⟨111⟩ axis by 180°. For comparison, we show in Fig. 1(a) the χ scan of the sample with the same thickness but without RTA. In this sample the type-*B* epitaxy is absent.

X-ray reflectivity results are shown in Fig. 2 for both 40 nm samples, with and without RTA. These curves show a large difference in roughness and in the true thickness of CaF_2 films. Qualitatively, the sample with RTA has a more abrupt interface as compared to the sample without RTA. The thicknesses were calculated using the spacing between Kiessig franges.[6] For the sample with RTA the true thickness is 26.3±0.2 nm, while the sample without RTA is 30.9±0.2 nm. This indicates that at the interface of the sample without RTA much less interdiffusion is present while RTA promotes a strong interdiffusion and probably reactions as well. In addition, x-ray diffraction ω scan results show a very low strain level for the sample without RTA (see Table I). A small broadening of the Si(111) peak observed in ω scans for the 40 nm sample with RTA show that the Si substrate is slightly expanded due to CaF_2 film on the top.

Figure 3 shows the calcium (Ca 2*p*) XPS spectra of the 40 nm samples with and without RTA near the interface. As the samples have different true thicknesses, as can be seen in

TABLE I. Full width half maximum (FWHM) of the Si(111) line for a wafer of silicon without film, for a 40 nm CaF_2 film without RTA and for a 40 nm CaF_2 film with RTA. The ω scans were performed using a Si(111) bulk crystal as the first crystal monochromator in a double axis diffractometer.

Samples	FWHM (arcsec)
Wafer-Si(111)	11.10
CaF_2(40 nm)/Si(111) without RTA	11.21
CaF_2(40 nm)/Si(111) with RTA	14.83

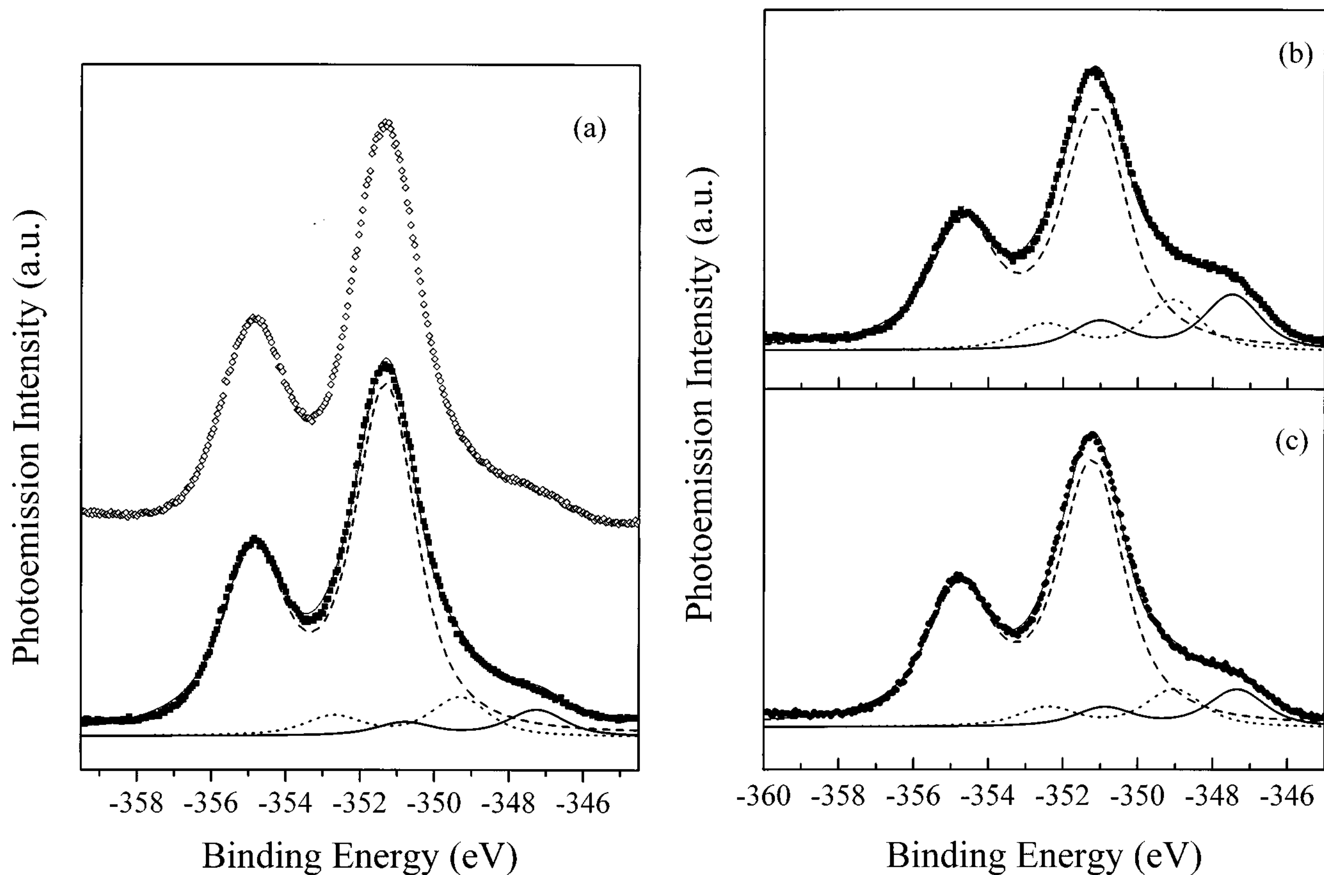

FIG. 3. Deconvoluted XPS spectra of 40 nm CaF_2 films. (a) Ca $2p$ spectra to samples with (○) and without (●) RTA for Ca/Si ratio is equal to 0.80 in both samples. (b) and (c) spectra with Ca/Si ratio equal to 0.24 for samples with and without RTA, respectively. In this figure the dashed line corresponds to Ca–F bonds, the doted line corresponds to Ca–O bonds and solid line corresponds to Ca–Si bonds.

x-ray reflectivity curves, we adopted the criteria of Hong and Dillingham,[7] who use the Ca/Si ratio to compare equivalent points in different samples. Figure 3(a) shows the XPS spectra at the same Ca/Si ratio in the samples at a point in front of the CaF_2/Si interface. Both samples present similar spectra with less evidence of bonding between Ca–O and Ca–Si. Using the same criteria, for a point after the CaF_2/Si interface, both the samples present a much more pronounced Ca–Si bonding. Therefore the samples with RTA present relatively 64% more Ca–Si bonds in comparison with the sample without RTA. These results are shown in Figs. 3(b) and 3(c). The depth profile (not shown) reveals that the interdiffusion layer is reduced by 40% in the sample with RTA, relative to the sample without RTA and the presence of 7 at. % Si at the surface of the sample with RTA.

Figure 4 shows the F/Ca ratio obtained by XPS profiling. This ratio increases 48% at the CaF_2/Si interface for the sample with RTA relative to the 40 nm sample without RTA. This indicated that half of Ca–F bonds present at the interface were broken. In contrast, the sample without RTA shows a relative decrease of about 6% at an equivalent point at the interface. This suggest that a fluorine evolution during the deposition of the sample without RTA can be occurring.

Figure 5 shows the TEM results. In the 40 nm sample with RTA [Fig. 5(b)], we find no grains in the otherwise smooth film. Misfit dislocations along the growth direction are clearly visible and we can estimate a dislocation density of about 10^{10} cm^{-2}. The inset [Fig. 5(f)] shows the SAED of the 10 μm^2 portion shown in Fig. 5(b) and we see a clear monocrystalline structure. By contrast, Fig. 5(a) shows an

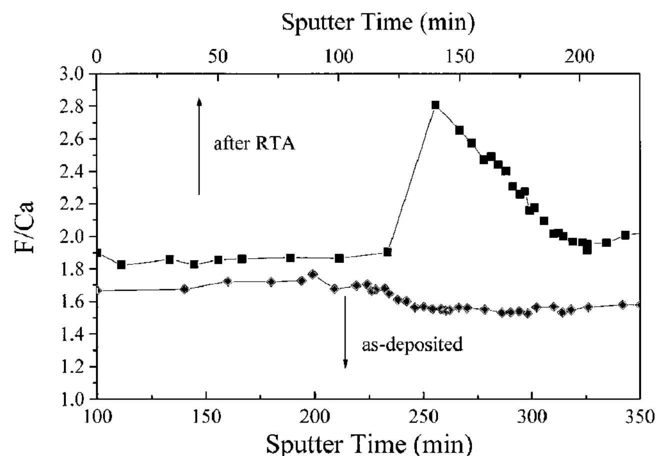

FIG. 4. Ratio of F/Ca concentrations sputter time for 40 nm samples with and without RTA. The top axis corresponds to the sample with RTA (square dots) and the bottom axis corresponds to the sample without RTA (diamond dots).

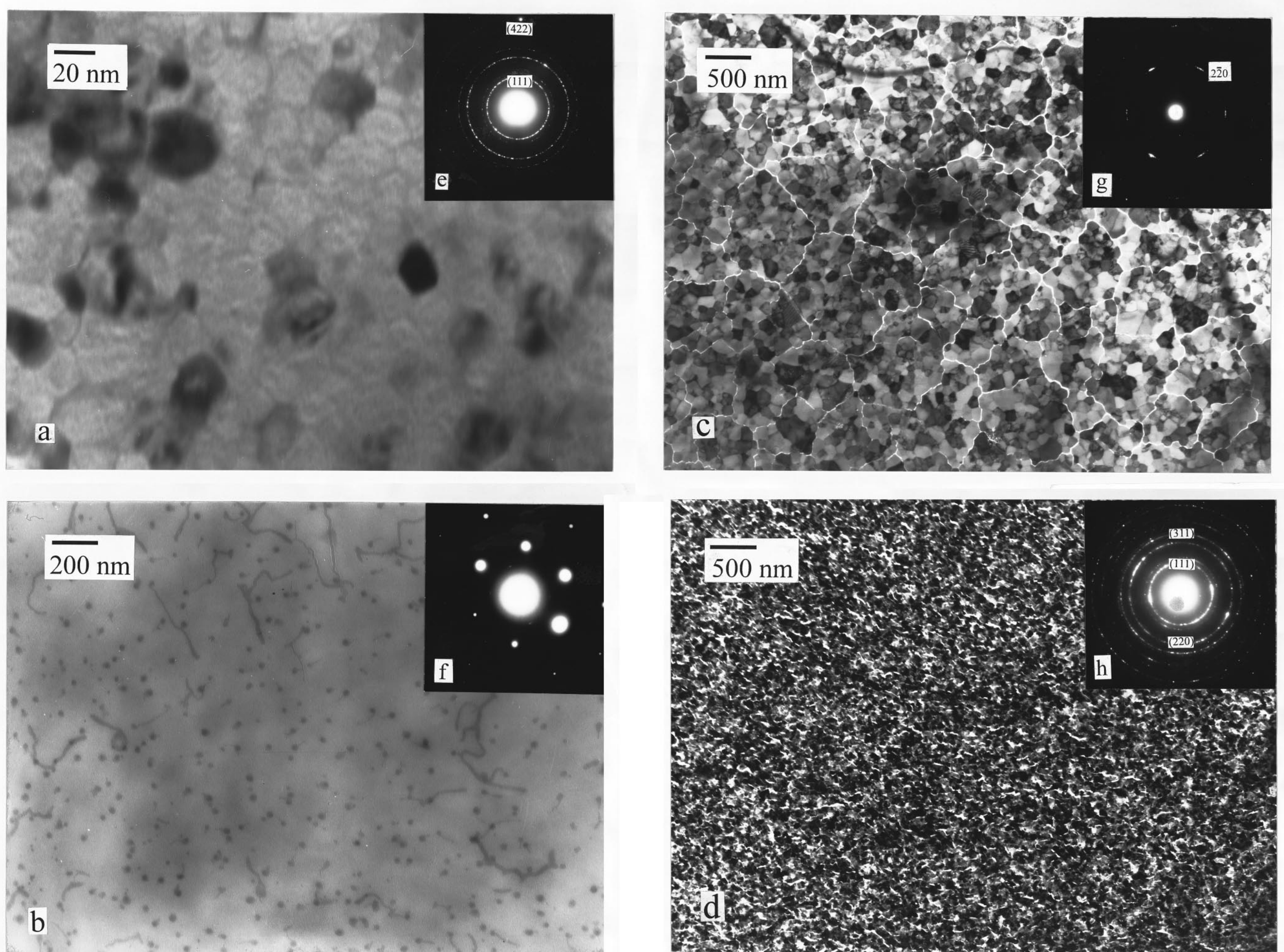

FIG. 5. TEM results for (a) 40 nm sample without RTA, (b) 40 nm sample with RTA, (c) 150 nm sample with RTA, and (d) 300 nm sample with RTA. (e), (f), (g), and (h) are the insets showing the selected area electron diffraction patterns of the main figures, respectively.

average grain size of around 24 nm for the 40 nm film without RTA, evidencing its polycrystalline character. The inset [Fig. 5(e)] shows the SAED of the portion displayed in Fig. 5(a) and we find a clear polycrystalline structure with a (111) texture as evidenced by the rings intensity. For the 150 nm sample with RTA Fig. 5(c) shows a morphology with grains and cracks. The average grain size is around 200 nm and the width of the cracks is of about 17 nm. The SAED of this sample [see Fig. 5(g)] shows fanlike decorated (220) spots. The average-angle value of this decoration is a fan of 9.5°. This angle represents the average angle of rotation between grains, characterizing a mosaic structure. For the 300 nm sample, we observe in Fig. 5(d) grains with an average size of 46 nm and cracks of about 23 nm. The insert, Fig. 5(h), shows the polycrystalline structure without an inplane texture. Table II shows the dependency of the average grain size with the film thickness.

IV. DISCUSSION

The application of RTA in CaF_2 films grown on Si substrates is well known. Pfeiffer *et al.*[8] use an *ex situ* RTA to obtain best quality CaF_2 films on Si(100). Singh *et al.*[5] have shown that best results are obtained when RTA is applied *in situ* at the deposition, i.e., without vacuum break, to CaF_2 films deposited on Si(111) at room temperature. Cho *et al.*[4] applied a thermal ramp in the first stage of the deposition, leading to a better quality of CaF_2 films compared to those obtained at low deposition temperatures. In our case, the samples are grown at 300 °C and after that they are submitted to RTA *in situ* at 1000 °C for 1 min by a halogen lamp situated at the back side of Si substrates. This characteristic RTA promotes a thermal pulse from the substrate to

TABLE II. Average grain size of CaF_2 films with and without RTA. The values of grain size were obtained by TEM micrographs and the thickness are nominal values used in the deposition.

Samples	Average grain size (nm)
CaF_2(40 nm)/Si(111) without RTA	24
CaF_2(40 nm)/Si(111) with RTA	>1000
CaF_2(150 nm)/Si(111) with RTA	200
CaF_2(300 nm)/Si(111) with RTA	46

the CaF_2 film. This thermal pulse produces mainly three effects in the CaF_2 films. First, the thermal pulse promotes a strong reaction between CaF_2 and Si at the interface as can be seen by the XPS results as well as by the x-ray reflectivity measurements. XPS analysis clearly show evidences of a Ca silicide formation, a partial consumption of original CaF_2 films, and an accumulation of fluorine at the interface. A reduction in the roughness at the interface by RTA is inferred by x-ray reflectivity measurements. Tromp and Reuter[3] reported on the presence of this Ca silicide with a bond length very close to the bond length of $CaSi_2$. Second, the TEM results show that RTA induces a morphologic change improving the polycrystalline structure to a single crystal structure. Generally, the increase of the sample thickness for the same thermal annealing produces a decrease in average grain size as well as in the crystalline quality, as can be seen in Table II. The microcracks observed in Figs. 5(c) and 5(d), not present in the 40 nm samples, can be explained by a reduction in elastic constants as a function of the thickness, using Karaninkas *et al.*[9] results on the basis of Brillouin light scattering measurements. Since the thermal pulse is the same for all samples, the presence of microcracks should be much more favorable to thin samples. The third effect is the stabilization of type-*B* epitaxy of the CaF_2 films due to the thermal pulse. The χ scan results clearly indicate that type-*B* epitaxy is absent in the as-deposited samples and present after RTA. In this aspect, Ohmi *et al.*[2] suggest a kind of potential barrier to explain the transition from type-*A* epitaxy to type-*B* epitaxy in their results. Now, we show in this work that type-*B* epitaxy can be reached even for low temperature deposited samples submitted to RTA. Possibly the energy of the thermal pulse associated with a Si diffusion is sufficient to break the CaF_2 bonds enhancing the Ca silicide formation, which give the necessary conditions to promote the transition of polycrystalline to single crystal type-*B* epitaxy.

V. CONCLUSIONS

We report on the effect of *in situ* RTA application on the structure and morphology by different techniques to CaF_2 films grown on Si(111). Our structural results show that films grown at low deposition temperatures can be single crystalline with type-*B* heteroepitaxy after an *in situ* RTA. The production of single crystals depends on the sample thickness which determines the propagation time of the isochronous thermal pulse. Furthermore, the application of RTA leads to sharper interfaces in comparison with as-deposited samples. In this process the formation of a Ca silicide is inevitable.

In summary, this study demonstrates that, in spite of the mostly phenomenological approach, the thermally induced diffusional flux and reaction near the CaF_2/Si interface can indeed contribute to the epitaxial mechanism. Therefore, further XPS research on CaF_2 films in the near future might include studies on duration of the applied thermal pulse as well as diffusional mechanism.

ACKNOWLEDGMENTS

This work was supported financially by PADCT/CNPq/PRONEX/MCT, CAPES, FBB and FAPERGS, Brazilian agencies. Thanks are due to Centro de Microscopia Eletrônica/UFPR for the TEM use access.

[1]L. J. Schowalter and R. W. Fathauer, CRC Crit. Rev. Solid State Mater. Sci. **15**, 367 (1989).
[2]S. Ohmi, K. Tsutsui, and S. Furukawa, Jpn. J. Appl. Phys., Part 1 **33**, 1121 (1994).
[3]R. M. Tromp and M. C. Reuter, Phys. Rev. Lett. **61**, 1756 (1988).
[4]C.-C. Cho, H. Y. Liu, B. E. Gnade, T. S. Kim, and Y. Nishioka, J. Vac. Sci. Technol. A **10**, 769 (1992).
[5]R. Singh, A. Kumar, R. P. S. Thakur, P. Chou, J. Chaudhuri, V. Gondhalekar, and J. Narayan, Appl. Phys. Lett. **56**, 1567 (1990).
[6]A. Naudon, J. Chihab, P. Goudeau, and J. Mimault, J. Appl. Crystallogr. **22**, 460 (1989).
[7]Y. Hong and T. R. Dilligham, J. Vac. Sci. Technol. A **11**, 2298 (1993).
[8]L. Pfeiffer, J. M. Phillips, T. P. Smith III, W. M. Augustyniak, and K. W. West, Appl. Phys. Lett. **46**, 947 (1985).
[9]J. M. Karanikas, R. Sooryakumar, and J. M. Phillips, J. Appl. Phys. **65**, 3407 (1989).